

Cross-correlators of conserved charges in QCD

R. Bellwied¹, S. Borsanyi², Z. Fodor^{2,3,4,5}, J. N. Guenther^{2,6}, J. Noronha-Hostler⁷, P. Parotto^{1,2}, A. Pásztor³, C. Ratti¹, J. M. Stafford¹

¹ Department of Physics, University of Houston, Houston, TX, USA 77204

² University of Wuppertal, Department of Physics, Wuppertal D-42119, Germany

³ Eötvös University, Budapest 1117, Hungary

⁴ Jülich Supercomputing Centre, Jülich D-52425, Germany

⁵ UCSD, Physics Department, San Diego, CA 92093, USA

⁶ University of Regensburg, Department of Physics, Regensburg D-93053, Germany

⁷ Department of Physics, University of Illinois at Urbana-Champaign, Urbana, IL 61801, USA

Abstract. We present cross-correlators of QCD conserved charges at $\mu_B = 0$ from lattice simulations and perform a Hadron Resonance Gas (HRG) model analysis to break down the hadronic contributions to these correlators. We construct a suitable hadronic proxy for the ratio $-\chi_{11}^{BS}/\chi_2^S$ and discuss the dependence on the chemical potential and experimental cuts. We then perform a comparison to preliminary STAR results and comment on a possible direct comparison of lattice and experiment.

Keywords: lattice QCD, heavy-ion collisions, freeze-out

Introduction and setup

The transition between hadronic matter and deconfined Quark Gluon Plasma (QGP) is a smooth crossover at vanishing baryon chemical potential [1,2,3,4], and is believed to turn into a first order transition for larger values of the chemical potential. Among the best suited observables for the study of the QCD phase diagram in the transition region are fluctuations of conserved charges. They can be studied in theory through first principles lattice QCD calculations (see e.g. [5,6,7,8,9]), as well as being closely connected to experimentally available measurements of net-particle fluctuations and correlations [10,11,12,13,14]. Due to the fact that some hadrons cannot be detected in experiment, a sizable share of B, Q, S is lost. Historically, the hadronic proxies used for B, Q and S are protons, the sum $p + \pi + K$ and the kaons themselves, respectively. More recently, the attention has moved towards non-diagonal correlators between conserved charges [13,14].

In this contribution we build a bridge between lattice-QCD-calculated correlators of conserved charges and experimentally accessible fluctuations and correlations of hadronic species, focusing on the correlator between baryon number and strangeness χ_{11}^{BS} . We employ the HRG model in order to include the effect

of resonance decays and cuts on the kinematics, which are present in the experiment. Most importantly, the HRG model allows us to isolate single particle-particle correlations and connect them to the correlators of conserved charges.

The ideal HRG model partition function is a sum over the single-state partition functions. Fluctuations of conserved charges are expressed as derivatives of the grand partition function with respect to the different chemical potentials:

$$\chi_{ijk}^{BQS}(T, \hat{\mu}_B, \hat{\mu}_Q, \hat{\mu}_S) = \frac{\partial^{i+j+k} (p/T^4)}{\partial \hat{\mu}_B^i \partial \hat{\mu}_Q^j \partial \hat{\mu}_S^k} = \sum_R B_R^i Q_R^j S_R^k I_{i+j+k}^R(T, \hat{\mu}_B, \hat{\mu}_Q, \hat{\mu}_S) , \quad (1)$$

where $\hat{\mu}_i = \mu_i/T$, and the phase space integral at order $i + j + k$ reads (note that it is completely symmetric in all indices, hence $i + j + k = l$):

$$I_l^R(T, \hat{\mu}_B, \hat{\mu}_Q, \hat{\mu}_S) = \frac{\partial^l p_R/T^4}{\partial \hat{\mu}_R^l} . \quad (2)$$

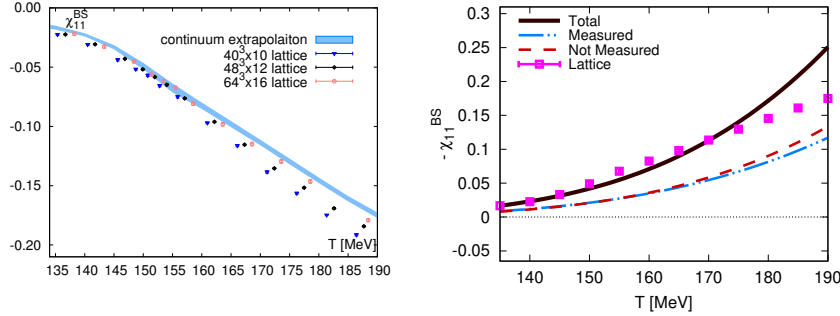


Fig. 1. The correlator χ_{11}^{BS} as a function of the temperature at $\mu_B = 0$. (Left panel) results for the ω_0 -based scale setting [15] at finite lattice spacing and continuum extrapolation. (Right panel) the continuum extrapolated results compared to HRG model calculations (solid black line), with the contribution from measured (dotted-dashed blue line) and non-measured (dashed red line) hadronic species. Figure from [16].

It is possible to recast the sum in Eq. 1 as a sum over the fewer states which are stable under strong interactions:

$$\sum_R B_R^l Q_R^m S_R^n I_p^R \rightarrow \sum_{i \in \text{stable}} \sum_R (P_{R \rightarrow i})^p B_i^l Q_i^m S_i^n I_p^R , \quad (3)$$

where $(P_{R \rightarrow i})^p$ is the average number of particles i produced by the decay of particle R .

The advantage of expressing the fluctuations in Eq. 1 in term of stable particles, is that we can further distinguish by particles which can be – or usually are – detected in experiment, and those which are not. In this work we employ the hadronic list labeled as PDG2016+ in [17], with the list of decays described and first utilized in [18]. We will hereafter consider the following species as the commonly measured ones:

$$\pi^\pm, K^\pm, p(\bar{p}), \Lambda(\bar{\Lambda}), \Xi^-(\bar{\Xi}^+), \Omega^-(\bar{\Omega}^+).$$

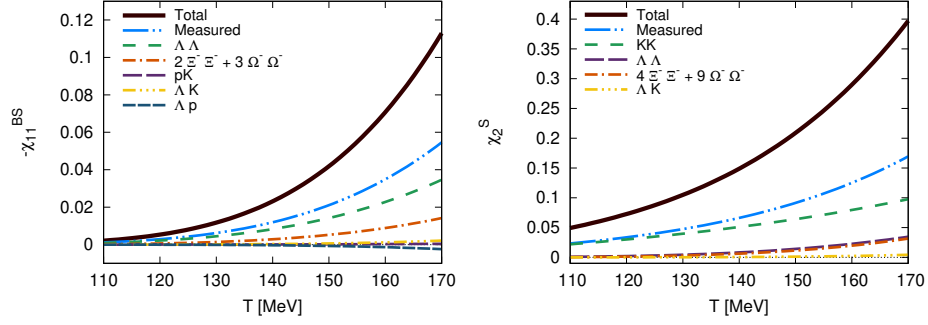


Fig. 2. Breakdown of the contributions from *measured* particle-particle correlators to $-\chi_{11}^{BS}$ (left panel) and χ_2^S (right panel), at $\mu_B = 0$, as a function of the temperature. Figure from [16].

In Fig. 1 we show the χ_{11}^{BS} correlator as a function of the temperature for vanishing chemical potential, calculated from the lattice (left panel) at different finite spacings, as well as its continuum extrapolation. In the right panel, along with the continuum extrapolation, we show the results from our HRG model analysis, where we separate the contribution to this correlator from measured and non-measured hadronic species. We see that the contributions roughly correspond to the same amount. Moreover, we can see in Fig. 2 the breakdown of the main contributions from *measured* particle-particle correlations to $-\chi_{11}^{BS}$ and χ_2^S at vanishing chemical potential.

Proxy for $-\chi_{11}^{BS}/\chi_2^S$

In order to perform a comparison to experiment and potentially to lattice QCD results, we consider the ratio $-\chi_{11}^{BS}/\chi_2^S$. Exploiting the information in Fig. 2, we construct the following proxy for this ratio:

$$\tilde{C}_{BS,SS}^{A,AK} = \sigma_A^2 / (\sigma_K^2 + \sigma_A^2) , \quad (4)$$

which is shown in the left panel of Fig. 3 as a blue dotted line, alongside the ratio $-\chi_{11}^{BS}/\chi_2^S$ (black solid line). This quantity well reproduces the full contribution for all temperatures around the QCD transition.

In Fig. 4 we show the same comparison for finite chemical potential, along parametrized chemical freeze-out lines with $T(\mu_B = 0) = 145, 165$ MeV. In the left panel we show the comparison in the absence of cuts on the kinematics, while in the central panel we introduce “exemplary” cuts, which are the same for all the hadronic species; in both cases we see that the proxy works well for a broad range of collision energies. In the right panel we compare our proxy in the case with and without the cuts, and notice that the effect of the cuts is quite modest. This hints at the possibility of directly comparing lattice QCD calculations and experimental measurements for this particular ratio.

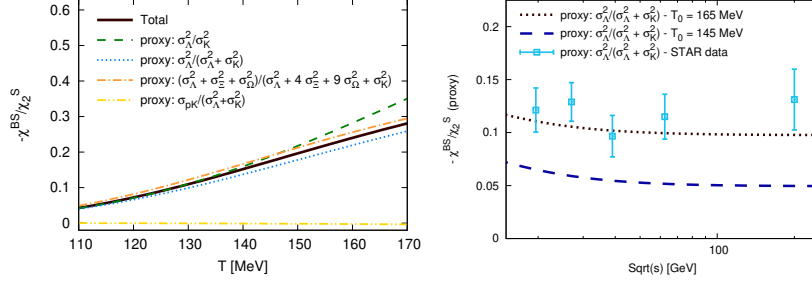


Fig. 3. (Left panel): comparison of different proxies (the proxy $\tilde{C}_{BS,SS}^{A,K}$ is shown as a blue dotted line) and the total contribution (black solid line) for the ratio $-\chi_{11}^{BS}/\chi_2^S$ at $\mu_B = 0$. (Right panel): comparison of our proxy with the kinematic cuts from [12,13], along parametrized freeze-out lines with $T(\mu_B = 0) = 145, 165$ MeV (black dotted and blue dashed). The STAR preliminary data are shown in light blue. Figure from [16].

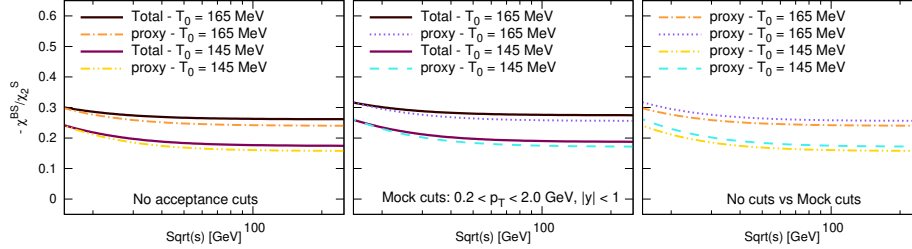


Fig. 4. Comparison of the proxy $\tilde{C}_{BS,SS}^{A,K}$ to the ratio $-\chi_{11}^{BS}/\chi_2^S$ for finite chemical potential, along the same freeze-out lines as in Fig. 3. The left panel shows the comparison without cuts, while the central panel with “exemplary” cuts. In the right panel the proxy is shown both with and without cuts. Figure from [16].

In the right panel of Fig.3 we compare preliminary STAR results to our proxy, where we have utilized the same cuts as present in the experimental analysis [12,13]. We see that a higher chemical freeze-out temperature is preferred, which is in line with previous findings [19,20]. A direct comparison to lattice QCD results is however premature, since it is essential that the same cuts are applied to all hadronic species for the proxy we constructed to reproduce the ratio $-\chi_{11}^{BS}/\chi_2^S$.

Acknowledgements

This project was partly funded by the DFG grant SFB/TR55 and also supported by the Hungarian National Research, Development and Innovation Office, NK-FIH grants KKP126769 and K113034. The project also received support from the BMBF grant 05P18PXFCA. Parts of this work were supported by the National Science Foundation under grant no. PHY-1654219 and by the U.S. Department of Energy, Office of Science, Office of Nuclear Physics, within the framework of

the Beam Energy Scan Theory (BEST) Topical Collaboration. A.P. is supported by the János Bolyai Research Scholarship of the Hungarian Academy of Sciences and by the ÚNKP-19-4 New National Excellence Program of the Ministry of Innovation and Technology. The authors gratefully acknowledge the Gauss Centre for Supercomputing e.V. (www.gauss-centre.eu) for funding this project by providing computing time on the GCS Supercomputer JUWELS and JU-RECA/Booster at Jülich Supercomputing Centre (JSC), and on SUPERMUC-NG at LRZ, Munich as well as on HAZELHEN at HLRS Stuttgart, Germany. C.R. also acknowledges the support from the Center of Advanced Computing and Data Systems at the University of Houston. J.N.H. acknowledges the support of the Alfred P. Sloan Foundation, support from the US-DOE Nuclear Science Grant No. de-sc0019175. R.B. acknowledges support from the US DOE Nuclear Physics Grant No. DE-FG02-07ER41521.

References

1. Y. Aoki, G. Endrodi, Z. Fodor, S. D. Katz and K. K. Szabo, *Nature* **443** (2006) 675 doi:10.1038/nature05120
2. S. Borsanyi *et al.* [Wuppertal-Budapest Collaboration], *JHEP* **1009** (2010) 073 doi:10.1007/JHEP09(2010)073
3. A. Bazavov *et al.*, *Phys. Rev. D* **85** (2012) 054503 doi:10.1103/PhysRevD.85.054503
4. A. Bazavov *et al.* [HotQCD Collaboration], *Phys. Lett. B* **795** (2019) 15 doi:10.1016/j.physletb.2019.05.013
5. S. Borsanyi, Z. Fodor, S. D. Katz, S. Krieg, C. Ratti and K. Szabo, *JHEP* **1201** (2012) 138 doi:10.1007/JHEP01(2012)138
6. A. Bazavov *et al.* [HotQCD Collaboration], *Phys. Rev. D* **86** (2012) 034509 doi:10.1103/PhysRevD.86.034509
7. A. Bazavov *et al.*, *Phys. Rev. Lett.* **109** (2012) 192302 doi:10.1103/PhysRevLett.109.192302
8. S. Borsanyi, Z. Fodor, S. D. Katz, S. Krieg, C. Ratti and K. K. Szabo, *Phys. Rev. Lett.* **111** (2013) 062005 doi:10.1103/PhysRevLett.111.062005
9. M. D’Elia, G. Gagliardi and F. Sanfilippo, *Phys. Rev. D* **95** (2017) no.9, 094503 doi:10.1103/PhysRevD.95.094503
10. L. Adamczyk *et al.* [STAR Collaboration], *Phys. Rev. Lett.* **112** (2014) 032302 doi:10.1103/PhysRevLett.112.032302
11. L. Adamczyk *et al.* [STAR Collaboration], *Phys. Rev. Lett.* **113** (2014) 092301 doi:10.1103/PhysRevLett.113.092301
12. L. Adamczyk *et al.* [STAR Collaboration], *Phys. Lett. B* **785** (2018) 551 doi:10.1016/j.physletb.2018.07.066
13. T. Nonaka [STAR Collaboration], *Nucl. Phys. A* **982** (2019) 863. doi:10.1016/j.nuclphysa.2018.10.092
14. J. Adam *et al.* [STAR Collaboration], *Phys. Rev. C* **100** (2019) no.1, 014902 doi:10.1103/PhysRevC.100.014902
15. S. Borsanyi *et al.*, *JHEP* **1209** (2012) 010 doi:10.1007/JHEP09(2012)010
16. R. Bellwied *et al.*, arXiv:1910.14592 [hep-lat].
17. P. Alba *et al.*, *Phys. Rev. D* **96** (2017) no.3, 034517 doi:10.1103/PhysRevD.96.034517

18. P. Alba, V. Mantovani Sarti, J. Noronha, J. Noronha-Hostler, P. Parotto, I. Portillo Vazquez and C. Ratti, Phys. Rev. C **98** (2018) no.3, 034909
doi:10.1103/PhysRevC.98.034909
19. R. Bellwied, J. Noronha-Hostler, P. Parotto, I. Portillo Vazquez, C. Ratti and J. M. Stafford, Phys. Rev. C **99** (2019) no.3, 034912
doi:10.1103/PhysRevC.99.034912
20. M. Bluhm and M. Nahrgang, Eur. Phys. J. C **79** (2019) no.2, 155
doi:10.1140/epjc/s10052-019-6661-3